Contents lists available at ScienceDirect

Colloids and Surfaces A: Physicochemical and **Engineering Aspects**

journal homepage: www.elsevier.com/locate/colsurfa



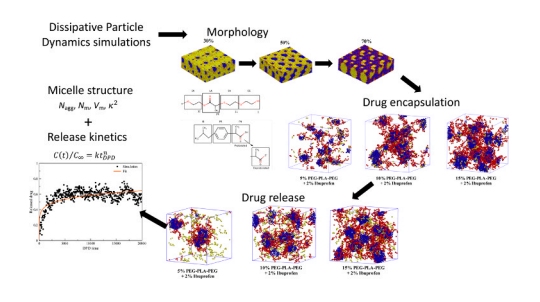


Investigation of morphology, micelle properties, drug encapsulation and release behavior of self-assembled PEG-PLA-PEG block copolymers: A coarse-grained molecular simulations study

Melike Merve Kuru ^{a,1}, Erdal Anil Dalgakiran ^{b,1}, Gokhan Kacar ^{a,b,c,*}

- ^a Department of Pharmaceutical Nanotechnology, Institute of Health Sciences, Trakya University, 22030 Edirne, Turkey
- b Department of Biotechnology and Genetics, Institute of Natural Sciences, Trakya University, 22030 Edirne, Turkey
- ^c Department of Genetics and Bioengineering, Faculty of Engineering, Trakya University, 22030 Edirne, Turkey

GRAPHICAL ABSTRACT



ARTICLE INFO

Keywords: Dissipative particle dynamics Coarse-grained simulations Drug delivery Block copolymers Micelle properties Colloids

ABSTRACT

Targeted drug delivery has become one of the key fields of personalized medicine. Developing candidate drug delivery agents requires a thorough understanding of the drug carrier materials by means of structure, drug encapsulation and release properties. To this aim, coarse-grained DPD simulations are employed to study the morphology, drug encapsulation and release of a particular amphiphilic block copolymer system. Extent of the drug encapsulation and release are observed to be mainly affected from copolymer concentration in the mixture. Mean aggregation number and average micelle volume are observed to increase as drug is encapsulated in the micelles. In addition, the shape of micelles is characterized as mainly spherical. It is observed that the drug release follows a pseudo-Fickian diffusion model and can be represented by the Korsmeyer-Peppas model. Furthermore, the diffusion rate of the drug molecules is observed to increase mainly in the release-phase. Our simulations can be viewed as a computational attempt to model the drug encapsulation and release by mimicking real experimental conditions, while yielding results on the structure and dynamics of the polymeric carrier. The results can be anticipated to find applications in understanding and controlling the parameters to design candidate drug delivery micelles at the molecular level.

^{*} Corresponding author at: Department of Genetics and Bioengineering, Faculty of Engineering, Trakya University, 22030 Edirne, Turkey. E-mail address: gokhankacar@trakya.edu.tr (G. Kacar).

 $^{^{1}\,}$ These authors contributed equally to the manuscript.

1. Introduction

Delivery of drugs to the targeted zone in the physiological environment has become one of the widely studied areas in nano-medicine research [1-5]. To achieve a proper drug delivery process, a huge variety of materials are being used from liposomes [6] to hydrogels [7], and from inorganic particles [8,9] to polymeric micelles [10-13]. The crucial points in designing prospective drug delivery micelles can be summarized as, to achieve the proper encapsulation of the drug, to properly release the cargo upon stimuli such as change in pH, enzyme concentration or redox gradients [14,15] and maintaining the stability of micelles [16,17]. In line with these objectives, polymeric micelles as drug delivery materials have gained tremendous attention due to their unique properties such as biocompatibility, high encapsulation efficiency, ability to be functionalized and increased solubility in water [18–23]. The presence of hydrophilic and hydrophobic units in a block copolymer chain leads to formation of spherical micelles at concentrations above their critical micelle concentration (CMC). These micelles. based on their chemical nature, have the ability to encapsulate hydrophobic drugs at their hydrophobic core or hydrophilic drugs at their hydrophilic core.

Investigation of the drug encapsulation and drug release properties of micelles is of utmost importance to improve the drug solubility, increase the drug circulation time, extend the drug residence time and finally to lead to the enhanced permeability and retention (EPR) effect [24,25] associated with the candidate drug delivery micelle. Therefore, studying micelle structure, and its relation to drug encapsulation and release properties are prominent in understanding the intrinsic properties in order to develop new drug delivery materials. Besides, a thorough understanding of the drug release process is required to evaluate the stability and drug carrying ability of a particular polymeric micelle. Recently, a great emphasis is given to design and develop drug delivery block copolymer systems with the ability to encapsulate and release drugs upon environmental stimuli [26–28].

In this work, we strive to perform dissipative particle dynamics (DPD) simulations to study the morphology, drug encapsulation and stimuli-responsive drug release properties of poly(ethylene glycol)-poly (lactic acid)-poly(ethylene glycol) (PEG-PLA-PEG) triblock copolymer micelles. The amphiphilic nature of the PEG/PLA system leads to the formation of spherical micelles [29]. Due to the biocompatibility, water solubility, nontoxicity and non-immunogenicity PEG is used as the hydrophilic block [30]. On the other hand, PLA is being used as the hydrophobic block in many cases due to its superior mechanical properties, low immunogenicity, biocompatibility and biodegradability [31]. Often, PEG and PLA are combined such that the hydrophobic groups form the head and tail sections of the block copolymer [32,33] or in diblock structures [34,35]. The morphologies of their diblock copolymers are investigated by Posocco et al. via mesoscopic simulations [36] and the self-organization of the former case is studied by Dolgov et al. [37]. In our case, the middle PLA block forms the hydrophobic core and has the ability to encapsulate the drug, ibuprofen. Ibuprofen is selected as the model hydrophobic drug to demonstrate our proposed simulation procedure in modeling the encapsulation and release properties. Ibuprofen is a poorly water-soluble drug. Therefore, this paper also aims to study a polymeric drug delivery medium, while bringing new insights on its morphology, structure and micellization properties to better understand the ibuprofen encapsulation and release properties.

Computational techniques are widely employed tools to study the drug encapsulation and drug release behavior of copolymeric micelles. Within the computational techniques such as molecular dynamics and coarse-grained simulations, dissipative particle dynamics (DPD) method steps forward as a widely employed coarse-grained simulation tool to study the drug encapsulation and release of drugs due to the inherent time-scales associated with the micelle formation, drug encapsulation and release [38,39]. The DPD method is recently used to simulate mostly pH-responsive drug delivery systems [40–43].

In this work, we use a realistic simulation procedure to model the encapsulation and release properties of the aforementioned system. By realistic, we refer to the computation of DPD interaction parameters between the functional groups of the copolymer and drug involving their proper chemistry-specific details. Moreover, we use a recent alternative DPD parameterization [44,45], where the bead volumes are dictated by their experimental volumes in contrast to the conventional DPD parameterization allowing equal bead-sizes. In addition, the affinity of PEG to water due to its hydrophilic nature is modeled by incorporating hydrogen bond interactions in DPD via a modified DPD potential [46]. By including these system-specific interactions, we present a simulation procedure to mimic the real experimental conditions that are relevant to the general field of drug delivery systems. In all, rather than a model computational study, where the encapsulation and stimuli-responsive release are defined by arbitrary assigned interaction parameters, our simulations incorporate the real chemical interactions in our modeling procedure.

We aim to characterize the morphologies at different concentrations, study the local interactions of hydrophilic and hydrophobic groups and the drug, and investigate the concentration effect on the drug encapsulation and drug release properties with a simulation-based procedure. Furthermore, we quantify the micelle properties such as mean aggregation number, average micelle volume and relative shape anisotropy to comment on the micellar structure as well. The results obtained in this work, could provide researchers tools to design new candidate drug delivery systems, which has improved encapsulation efficiency and release properties.

2. Simulation details and materials

2.1. DPD simulation method

DPD is an off-lattice, coarse-grained simulation method that operates at the meso-scale. By the coarse-graining procedure, chemical functional groups of block copolymer and drug are represented as molecular entities referred as *beads*. DPD is first proposed by Hoogerbrugge and Koelman [47] as an improvement to lattice gas automata [48] to study fluid mechanics problems. Later, Groot and Warren [49] improved DPD method to compute the mesoscopic DPD interactions from Flory-Huggins mean field theory [50]. This improvement has allowed DPD to be applicable to complex soft materials such as polymers, lipids and biopolymers [51]. In DPD, the motion of the coarse-grained particles is governed by Newton's equations of motion.

The total force acting on a single DPD bead \mathbf{f}_i is composed of three types of forces, namely conservative force \mathbf{F}^C_{ij} , dissipative force \mathbf{F}^D_{ij} , and random force \mathbf{F}^R_{ij} . The overall end-structure is characterized by the conservative force, which contains the non-bonded contribution of the total potential energy of the system. For the bonded interactions, a harmonic force \mathbf{F}^H_{ij} between bonded beads is added to the total force, which becomes

$$\mathbf{f}_i = \sum_{i \neq j} (\mathbf{F}_{ij}^C + \mathbf{F}_{ij}^D + \mathbf{F}_{ij}^R + \mathbf{F}_{ij}^H). \tag{1}$$

The mathematical forms of the conservative, dissipative and random forces read as

$$\mathbf{F}_{ij}^{C} = \begin{cases} a_{ij} (1 - r_{ij}/R_{c}) \hat{\mathbf{r}}_{ij} & r_{ij} < R_{c} \\ 0 & r_{ij} \ge R_{c} \end{cases} ,
\mathbf{F}_{ij}^{D} = -\gamma \omega^{D}(r_{ij}) (\hat{\mathbf{r}}_{ij} \mathbf{v}_{ij}) \hat{\mathbf{r}}_{ij},
\mathbf{F}_{ij}^{R} = \sigma \omega^{R}(r_{ij}) \theta_{ij} \hat{\mathbf{r}}_{ij}$$
(2)

where, a_{ij} is the strength of the repulsive interaction between bead types i and j, $\mathbf{r}_{ij} = \mathbf{r}_i - \mathbf{r}_j$, $r_{ij} = |\mathbf{r}_{ij}|$, and $\hat{\mathbf{r}}_{ij} = \mathbf{r}_{ij}/|\mathbf{r}_{ij}|$. For the dissipative and random forces, $v_{ij} = v_i - v_j$. The $\omega^D(r_{ij}) = [\omega^R(r_{ij})]^2$ and

 $\omega^R(r_{ij})=1-r_{ij}/R_c$ are the weight functions that are functions of the interparticle distance r_{ij} and become zero at the cut-off distance R_c . $\sigma^2=2\gamma k_BT$ and θ_{ij} is the randomly fluctuating variable with Gaussian statistics. In our simulations, we adopt the values from Groot and Warren for the γ parameter reading as 4.5 [49]. The harmonic force $\mathbf{F}^H_{ij}=\sum C_S(r_{ij}-r_{ij,0})$, where C_S is the spring constant between bonded beads and $r_{ij,0}$ is the equilibrium bond distance, which are set to $10~k_BT/r^2_{\rm DPD}$ and $0.5~r_{\rm DPD}$, respectively.

The non-bonded DPD interactions are soft, purely repulsive and originally developed for beads having similar sizes as a consequence of Flory's mean field theory [50]. In our simulations, we use a parameterization to compute the parameter a_{ij} , where the local volumes around beads are dictated by their pure liquid densities yielding the proper experimental bead sizes in the simulations [45] via

$$a_{ij} = \widehat{a}_{ij} + \frac{p}{0.0454(a_{ii}\rho_{i,pure} + a_{jj}\rho_{j,pure})}\chi_{ij}k_BT,$$

$$\widehat{a}_{ij} = \sqrt{a_{ii}a_{jj}},$$

$$a_{ii} = \frac{p - \rho_{i,pure}k_BT}{a\rho_{i,pure}^2r_{DPD}^3} \text{ and } \alpha = 0.101.$$

$$(3)$$

In Eq. (3), a_{ii} and a_{jj} are the repulsion strength values between same type of beads, \widehat{a}_{ij} is defined as the neutral interaction parameter yields zero repulsion upon mixing of i and j beads, and ρ_i is the dimensionless number density of the pure component i. The Flory-Huggins interaction parameter χ_{ij} [50] quantifies the degree of mixing between beads and is computed from the experimental solubility parameters δ by the following relation:

$$\chi_{ij} = \overline{V}(\delta_i - \delta_j) / k_B T. \tag{4}$$

In Eq. (4), \overline{V} represents the average volume of a particular bead in the simulations computed from the average density from $\overline{V} = \rho^{-1} = \left(\sum_{i} N_{i} \rho_{i,\text{pure}}^{-1}\right) / \sum_{i} N_{i}$.

In our simulations, we treat the hydrogen bond interactions between hydrophilic groups of the copolymer (EA and EG beads), specific sections of the drug (FN bead) and water as a separate force term added to the total force in DPD. The main reason is that the pure repulsive interactions and the soft non-bonded potential of DPD is not able to represent the attractive interactions for systems, where the hydrogen bonds are dominant. The separate term is in the form of a Morse type interaction in the form of,

$$V_{Morse} = e_{HB} \left[e^{-2\sigma(r - r_0)} - 2e^{-\sigma(r - r_0)} \right] \quad r < r_{DPD}.$$
 (5)

In Eq. (5), e_{HB} is the hydrogen bond strength, σ is the curvature of the potential and r_0 is the equilibrium hydrogen bond distance value. The parameters of the Morse potential are adopted from our previous work by a fitting to the physical properties of PEG beads [46]. In our modeling procedure of hydrogen bonds, we do not explicitly consider the directionality. The reason is that the formation/dissociation times of hydrogen bonds are much lower than the DPD time [46]. Nevertheless, our hydrogen bonding procedure is capable of representing the three-dimensional tetrahedral structure of water as computed from the three-body angular distributions as reported before [52]. Moreover, the reason for taking similar hydrogen bond strength of the FN bead (*i.e.*, propinoic acid) as alcohols is that low molecular weight acids has similar affinities to water [53].

Incorporating the variable bead sizes and hydrogen bonds in DPD is previously employed by our group to model ibuprofen encapsulation in poloxamer micelles with a good prediction of the experimental structural and drug encapsulation properties [54].

2.2. Coarse-graining of copolymer and drug molecules

In this work, we study the block copolymer system PEG-PLA-PEG to simulate the phase behavior, structure, drug encapsulation and drug release properties. Ibuprofen is used as the model drug due to the simplicity of its chemical structure. The self-assembly behavior of the copolymer was previously studied and spherical micelles were experimentally obtained [29]. The block copolymer system is taken from the experimentally synthesized version, where the number of repeating units of the monomers reads as $\rm EA_{12}LA_{29}EA_{11}EG_1$ [29]. Ibuprofen is composed of three beads, namely IB, PR and FN. The chemical structures, the coarse-graining with the number of repeating units of copolymer and the drug molecule are depicted in Fig. 1.

The coarse-graining of the copolymer and the model drug ibuprofen results in the formation of beads as demonstrated in Fig. 1. Each bead is capped with the proper number of hydrogen atoms in order to form a neutral bead. There are three types of beads forming the copolymer and each refers to a different chemical structure: EA and EG represent hydrophilic and LA represents hydrophobic parts. In order to incorporate the -OH group at the end of the chain bead type EG is defined. The coarse-graining of the ibuprofen drug is done for two scenarios in our study: Initially, a protonated FN bead corresponding to neutral conditions is used in the drug encapsulation process, and later a deprotonated FN bead is defined since the carboxyl group -COOH is expected to be deprotonated in the physiological environment, where the drug release process takes place [55].

2.3. DPD simulation details

The simulations performed in this work can be divided to three sets: In the first set, we run drug-free simulations at different copolymer weight percent values to investigate the phase behavior and morphologies of the PEG-PLA-PEG copolymer system in an aqueous environment. As the second step, we construct the simulation boxes to simulate the drug encapsulation process. The encapsulation simulations are performed by considering an initial structure, where all beads are scattered within the simulation box randomly. Therefore, encapsulation of the drug beads is realized while self-assembling process takes place. The neutral ibuprofen molecule parameters are used for the drug encapsulation process. For the final step, we simulate the drug release process by using the structures that are formed in step two. In other words, the final simulation snapshots of the drug encapsulated systems are used as input coordinates to the drug release simulations.

As mentioned before, the release of drug molecules takes place at the physiological conditions, where experimentally the carboxyl group becomes the negatively charged carboxylate group upon deprotonation of the -COOH group. It is reported in literature that the charged groups have extra affinity to neutral water molecules [56,57] and the presence of ions in the system increases hydrogen bond strength of water [58] with significant change in dynamics [59]. In the case of ibuprofen, the water solubility increases by a factor of about 100 upon deprotonation [60]. In our DPD simulations, we do not employ electrostatic interactions as a result of the negative charge present in the carboxylate group. Instead, we mimic the extra affinity of carboxylate group to water by increasing the strength of the hydrogen bond between the deprotonated FN bead and the solvent water beads. The hydrogen bond strength between the deprotonated FN bead is increased by a factor 5 difference compared to the protonated FN bead. All of the -COOH groups in the system are deprotonated and new set of simulation parameters are used in the simulations to model the release process. A factor 5 difference between the protonated and deprotonated FN beads is selected since with this value, a maximum drug release from a particular copolymer is attained in the simulations. The details of the selection of the hydrogen bond strength and the rest of the simulation parameters are given in Supplementary Material.

The DPD simulations are performed with the LAMMPS package [61,

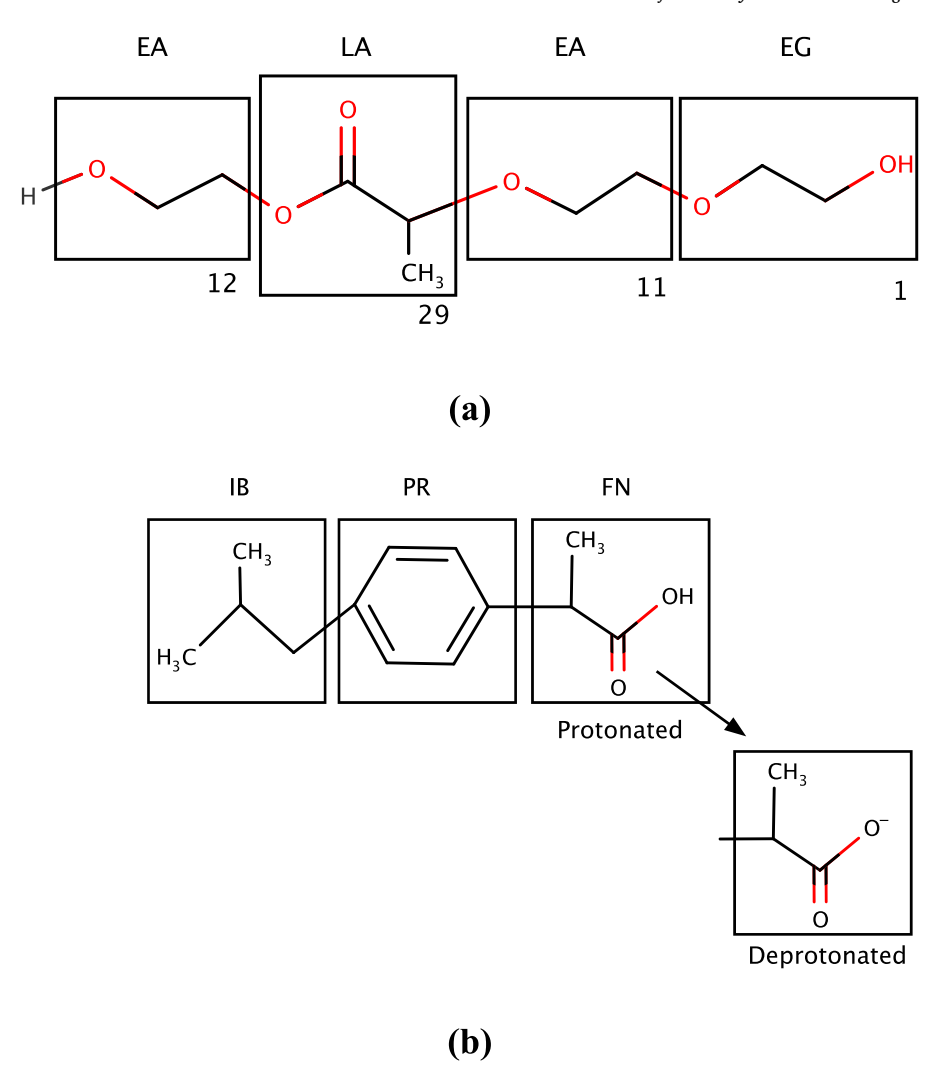


Fig. 1. Chemical structures and the coarse-grained beads of (a) PEG-PLA-PEG copolymer and (b) model drug ibuprofen. Numbers indicate the number of repeating units as similar to the experimental system in Ref. [29].

62]. The initial structures are created with the Scienomics MAPS v4.3 software [63]. In all simulations, the total number of beads in the simulation box are kept constant for all simulations and set to 81,000. The number of beads corresponding to the copolymer, water and drug beads are adjusted to correspond to the set weight percent values. In all cases, the beads are distributed randomly irrespective of their type in the simulation boxes at the beginning of the simulation. The total number of beads in the box results in a periodic simulation box dimensions of 30 \times $30 \times 30 r_{DPD}^3$ for a number density value of 3. A similar simulation box volume is chosen previously by Droghetti et al. to validate the phase diagram and study the clustering of a poloxamer system [64]. In their work, they tested different box lengths from $20 \times 20 \times 20$ to $40 \times 40 \times 40$ in r_{DPD}^3 units and observed that a selection of a box length $30 \times 30 \times 30$, such as in our case, is reasonable in reducing the simulation box artefacts and reaching suitable simulation times. The time step values in the simulations for the drug-free and drug encapsulation simulations are set as 0.02 $t_{\rm DPD}$. A smaller time step value of 0.005 $t_{\rm DPD}$ is selected for the drug release simulations to stabilize the energy increase as a result of the increase in the hydrogen bond strength. For each part (namely, drug-free, drug encapsulation and drug release) the total time step of simulations is set as 10^6 DPD steps. The initial 8×10^5 steps of each part are used for equilibration and the last 2×10^5 for data collection. As mentioned earlier, drug encapsulation and drug release simulations are performed as consecutive steps, where the final snapshot of drug

encapsulated system is used as input to drug release simulations. An estimation of the real simulated time can be done by using the time scale as obtained in Groot and Rabone's work [65], where 1 $t_{\rm DPD}$ is about 14 ps. This makes the total real time in our simulations of about 280 ns. In the simulations, *NVT* conditions are used with the reduced temperature value of 1 $k_{\rm B}T$.

The drug encapsulation efficiency (DEE) values are estimated by an in-house developed code, counting the number of ibuprofen beads that are in contact with the micelles. In our computation, if the distance between the ibuprofen and copolymer beads is below a pre-defined cutoff value (*i.e.*, $1\,r_{\rm DPD}$), then the ibuprofen is considered as encapsulated. This approach to compute the DEE previously led to a proper estimation of experimental DEE values [54].

3. Results and discussion

3.1. Effect of PEG-PLA-PEG copolymer concentration on morphologies

We initially perform DPD simulations of the copolymer in water environment in order to observe the formation of self-assembled micelles and study the morphology as affected by increasing copolymer concentration. The concentrations are reported in copolymer weight percent values. We simulate 7 different concentrations that read as 5%, 10%, 15%, 30%, 50%, 70% and 90%. 5% is selected as the starting configuration since it corresponds to a concentration (*ca.* 53.1 g/L) that

is much higher than the experimentally obtained critical micelle concentration (CMC) value for the similar systems (i.e., 0.05–0.1 g/L) [29, 66]. In principle, CMC can be estimated from DPD simulations from alternative methods such as, in Neimark et al., where the free surfactant concentration in the solvent is used to estimate the CMC [67] or in Anderson et al., where the CMC is determined from the relation of the free surfactant concentration to the increasing total surfactant concentration [68]. In our work, we do not attempt to computationally determine the CMC since it is beyond the scope of this paper.

The first three copolymer concentrations, namely, 5%, 10% and 15%, are observed to yield spherical micelles in Fig. 2. As expected, the hydrophilic groups of the block copolymer (bead types EA and EG) construct the corona part of the micelles as a result of their affinity against water. In contrast, the hydrophobic groups (bead type LA) form the core of the micelles.

As the copolymer concentration is increased in the system, the micelle size is observed to increase as seen in Fig. 2. As the copolymer weight percent set to 30%, the micelles are visible in the form regular spherical micelles and irregular shaped micelles. The irregular shaped micelles form after some of the micelles are fused together. At 50%, the copolymer structure becomes somewhat perforated due to the presence of water trapped in between copolymer-rich domains. The perforated lamellar structure with an onset of a reverse-micellization process is noted at 70% copolymer. Finally, at 90%, a reverse-micelle formed structure is clearly visible.

The micelle-forming weight percent values that are obtained in our drug-free simulations are selected to proceed with the drug-loading simulations, namely 5%, 10% and 15%. By drug-loading, we refer to the amount of drug beads inside a particular simulation box. Each micelle forming system is studied with three different drug weight percent values of 0.1%, 1% and 2% of the whole system making up a total of 9 different systems. The drug amounts in the simulations are in line with the experimental concentration range [69,70]. In the following sections, we perform DPD simulations to study the drug encapsulation and release processes and quantify the structural and micellar properties as affected thereof.

3.2. Effect of drug encapsulation and release on copolymer and drug interactions

Initially, we study the interactions between the copolymer micelles and the drug molecules. The interactions are quantified from the obtained structures and are characterized by computing the radial distribution functions (RDF) g(r) by the following relation:

$$\frac{g_{ij}(r) = \left\langle \Delta N_{ij}(r \to r + \Delta r) \right\rangle V}{4\pi r^2 \Delta r N_i N_j} \tag{6}$$

where, the $\langle \Delta N_{ij}(r \rightarrow r + \Delta r) \rangle$ part gives the average number of j beads around i beads in a shell that is from r to $r + \Delta r$. V is the volume of the system and N is the number of beads.

We discuss the interactions of copolymer sub-units, namely hydrophilic and hydrophobic, and the drug molecules. The RDFs are plotted with respect to the changing drug amounts in the mixture. Although, ibuprofen is a hydrophobic drug it has a slight affinity to water due to the presence of the neutral carboxyl group (FN bead) as discussed earlier. In Fig. 3, the RDF plots of hydrophilic groups of the copolymer and drug molecules are depicted. Therefore, we notice a minor attraction of the hydrophilic groups to ibuprofen, which is evident by the first RDF peaks in all copolymer ratios. Moreover, the decrease of the second peak of the RDFs as the copolymer ratio in the mixture is increased, means a decrease of interactions at larger distances. On the other hand, the widening of the second peak can be associated with the enlarged micelle sizes (see, Table 1).

The RDF profiles in Fig. 4 clearly indicate a significant degree of interaction between the hydrophobic part of the copolymer and the drug

molecules as a result of the hydrophobic effects visible as higher first RDF peaks. However, these interactions are somewhat shorter-ranged as compared to the hydrophilic part and ibuprofen interactions due to the presence of a fast decay of the RDFs. A short-range interaction of the hydrophobic beads and the drug is expected due to the hydrophobic nature of ibuprofen, which leads accumulation of the drug near the core of the micelle. Apart from the decrease in the peak heights, a slower decay of the RDFs is noticed as the copolymer concentration is increased. This is, again, an outcome of the enlarged micelle sizes as the copolymer content is increased (see, Table 1). Nevertheless, although the increasing drug concentration at a particular copolymer concentration leads to a slight change in the first peak values of the RDFs, the overall behavior is qualitatively quite similar. This is also the case in the hydrophilic-drug bead interactions.

We compute the RDFs to comment on the structure of the drug release simulations as well. Again, we plot the RDFs for hydrophilic beads and hydrophobic beads with regard to the drug beads in Figs. 5 and 6.

The release of the drug from the micelles apparently influences the interactions between the hydrophilic groups of the copolymer and the drug. In Fig. 5, we notice a significant decrease of the first RDF peaks for all systems as compared to the drug encapsulation simulations in Fig. 3. This means that the drug beads move farther away from the hydrophilic groups towards the water environment. On the other hand, the less pronounced second peak of the RDFs in Fig. 5 as compared to Fig. 3 is the result of decrease of interactions of the copolymer hydrophilic groups and the ibuprofen.

Although, the first RDF peaks in Fig. 6 are decreased significantly as compared to Fig. 4, the hydrophobic groups of the copolymer and the drug molecules are still interacting in the drug release simulations, since there are still some drug molecules present at the hydrophobic core of the micelles with varying concentrations. This varying concentration depends on how much, on average, the drug is released in a particular system. The difference in between RDF profiles quantifying the interactions of the hydrophobic groups and the drug is seemed to be correlated with the DEE value after the release process takes place, which are tabulated in Table 4. The more the DEE value after the release of a particular system, the more the hydrophobic copolymer beads and the drug is interacting, and vice versa. For example, within the 5% copolymer simulations, the highest DEE value after the release is encountered for the 0.1% ibuprofen loading, where the corresponding first RDF peak is the minimum. The decreasing sequence of RDF peaks are in line with the DEE values after the release of this system. This conclusion is true for the 10% and 15% copolymer concentrations.

3.3. Effect of drug encapsulation and release on micelle properties

The simulation snapshots give us an exemplary overview of the qualitative aspects of the drug encapsulation process. The simulation snapshots of the drug encapsulation simulations are depicted in Fig. 7 with respect to a particular drug loading value for all copolymer weight percent values. Snapshots for the rest of the systems are demonstrated in Fig. S2 of the Supplementary Material.

The simulation snapshots as presented in Fig. 7 and in Fig. S2 yield insights on the encapsulation of ibuprofen and structure of PEG-PLA-PEG micelles. The systems containing the least number of drug molecules (namely, 0.1% ibuprofen loading in Fig. S2), we notice only a few spots of accumulated drug beads near micelles indicating that not all of the micelles encapsulate the drug due to the limited number of ibuprofen beads in the simulation box. In addition, the drug beads are positioned at the surface of the hydrophobic core rather than engulfed in-depth (see, Fig. S8 of Supplementary Material). This conclusion is consistent with the DEE values of the encapsulation simulation as tabulated in Table 4. Moreover, as we increase the copolymer concentration in the system, we see that the micelles enlarge and occupy larger volumes in the simulation box as will be discussed in the following paragraphs.

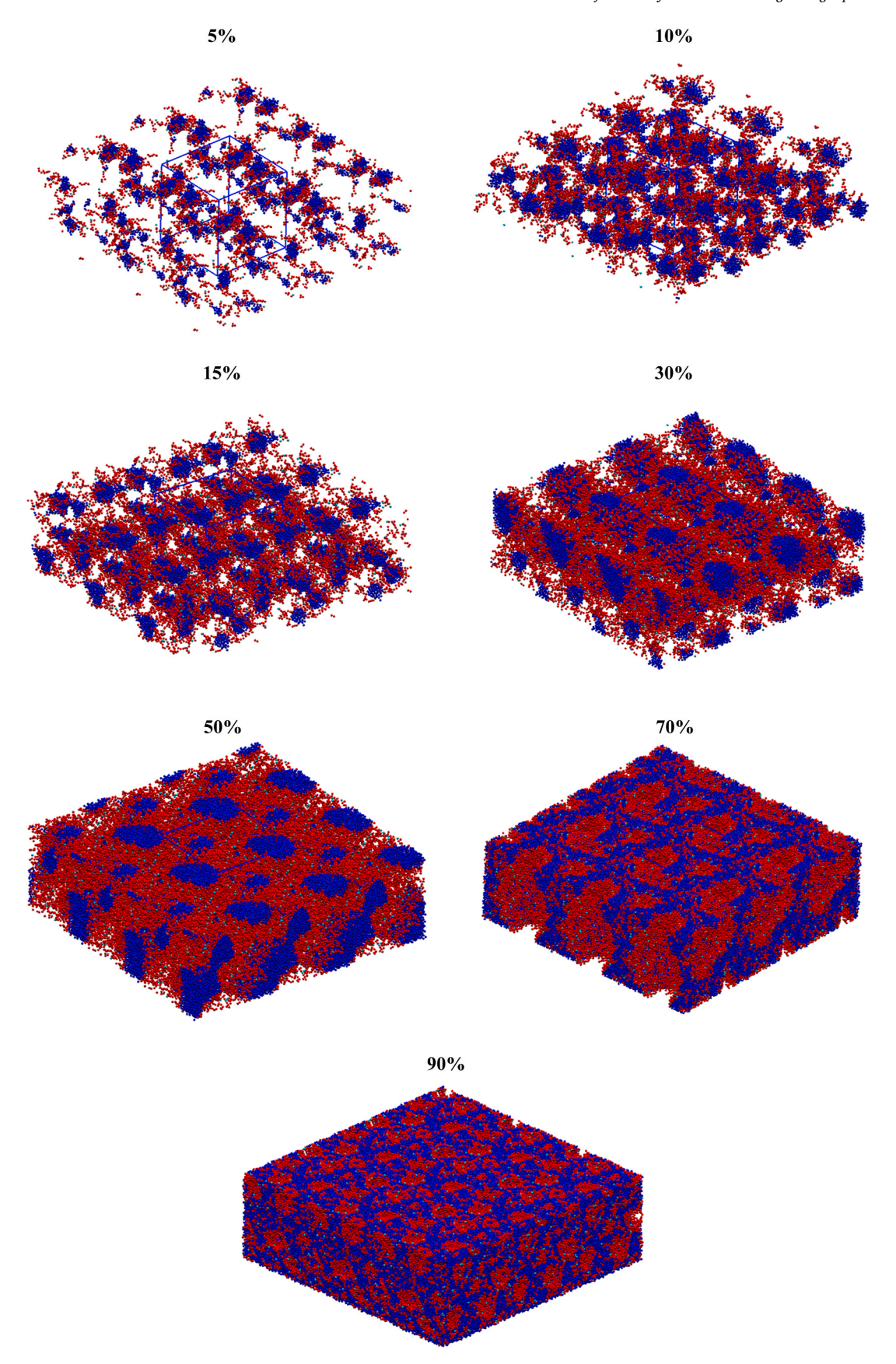


Fig. 2. Morphologies of PEG-PLA-PEG copolymers at different concentrations in aqueous solution. Red and blue colors indicate bead types EA and LA, respectively. The periodic simulation box lies in the middle section of the square and is repeated in different dimensions for a better visualization of the structure. Percentage values are the weight percent of the PEG-PLA-PEG copolymer in aqueous solution. The same simulation snapshots with visible water beads are presented in the Supplementary Material. (For interpretation of the references to color in this figure legend, the reader is referred to the web version of this article.)

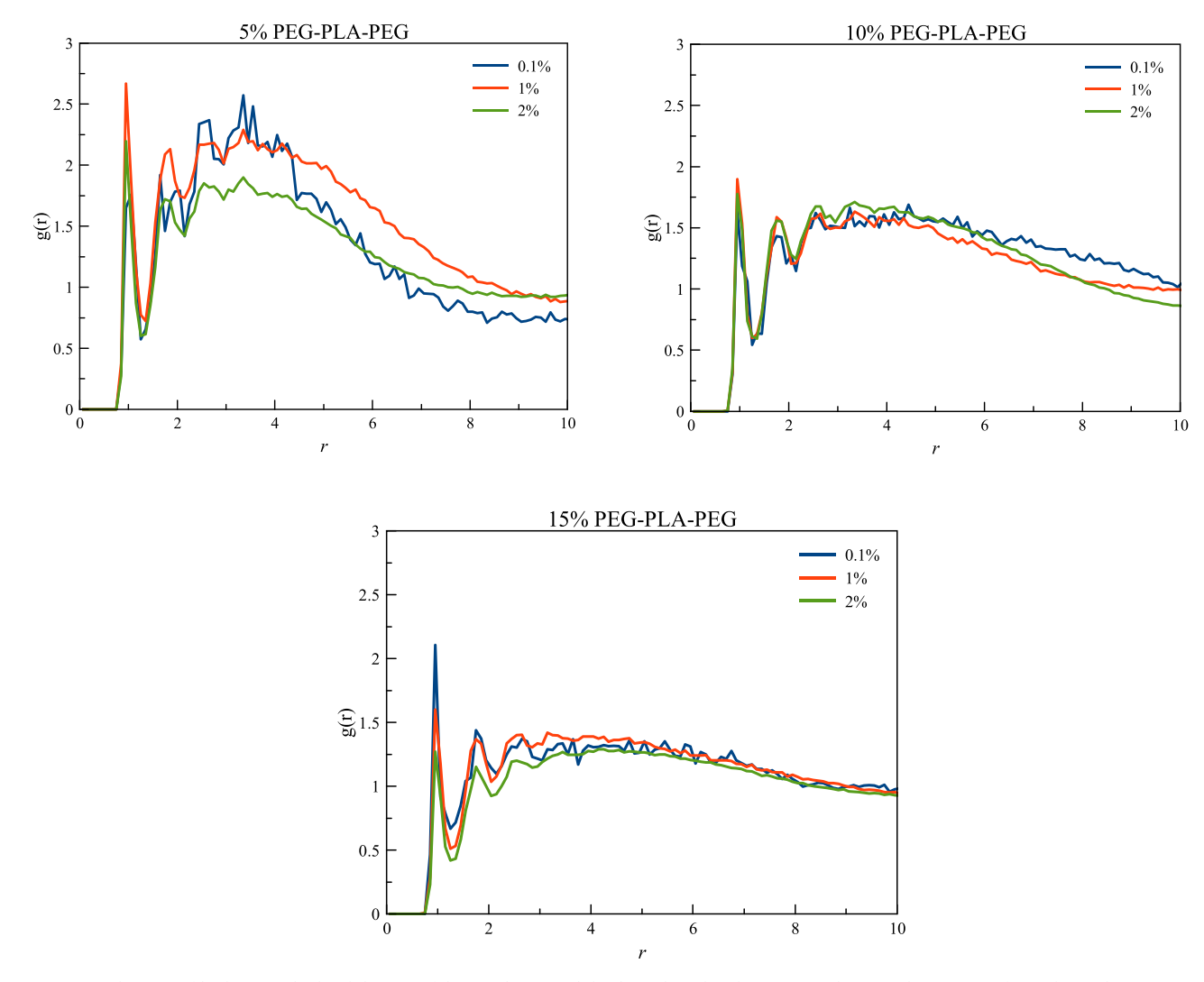


Fig. 3. Computed RDF profiles between hydrophilic part of the copolymer and the drug plotted with respect to changing drug content for each copolymer ratio in the system for drug encapsulation simulations. Distances are in DPD units r_{DPD}.

Table 1 Mean aggregation number $N_{\rm agg}$ computed for every simulated system. Only final snapshot is considered. The errors are associated with $N_{\rm agg}$ are the standard error of the mean. The values in parentheses are the number of micelles $N_{\rm m}$ in a simulation box.

	No drug	Encapsulation			Release		
		0.1%	1%	2%	0.1%	1%	2%
5%	3.3±0.7 (6)	2.8±0.4 (8)	6.3±1.3 (4)	3.4±0.5 (7)	6.3±1.3 (4)	8.3±0.7 (3)	8.3±0.7 (3)
10%	4.8±0.8 (10)	8.3±0.9 (6)	8.3±2.1 (6)	10.0±1.1 (5)	8.3±0.9 (6)	8.3±2.1 (6)	10.0±1.1 (5)
15%	$6.8{\pm}1.2$ (11)	8.6±1.5 (9)	11.0±1.6 (7)	11.0±1.7 (7)	9.6±1.5 (8)	11.0±1.6 (7)	11.0±1.7 (7)

Similarly, it is shown in Fig. 8 (and in Fig. S3 in the Supplementary Material) that there is a significant degree of drug release takes place as the simulation snapshots are compared to the drug encapsulation simulation snapshots. The ibuprofen beads in Fig. 8 are observed to be present outside of the micelles due to their increased attraction to the solvent, water. The simulation boxes are clearly more crowded by means of micelles for the 10% and 15% copolymer systems compared to the 5% copolymer system. Therefore, the diffusion of the ibuprofen beads to the solvent environment is more preferable for the 5% copolymer system due to the more copolymer-free space. This conclusion is true if the diffusion constant values of the 5% system as reported in Table 5 are compared to the rest of the systems for the encapsulation simulations.

A clearer picture arises when the micelle properties are quantified.

Therefore, we compute and discuss the micelle properties by means of their mean aggregation number $N_{\rm agg}$, number of micelles $N_{\rm m}$, average micelle volume $V_{\rm m}$ and relative shape anisotropy κ^2 as computed for each simulated system. The mean aggregation number indicates the number of chains that form a particular aggregate. In our calculation, an aggregate is considered to be formed from the presence of at least 2 block copolymer chains. In Table 1, we tabulate the computed $N_{\rm agg}$ together with the number of micelles for each system. We use the same notation for aggregates and micelles since our simulated concentrations are above the CMC as discussed earlier. The values are computed for different cases such as, for the system with no drug, the system after drug is encapsulated and the system after a portion of the drug is released (i.e., diffused out of the micelles). It is assumed that the chain exchange rate

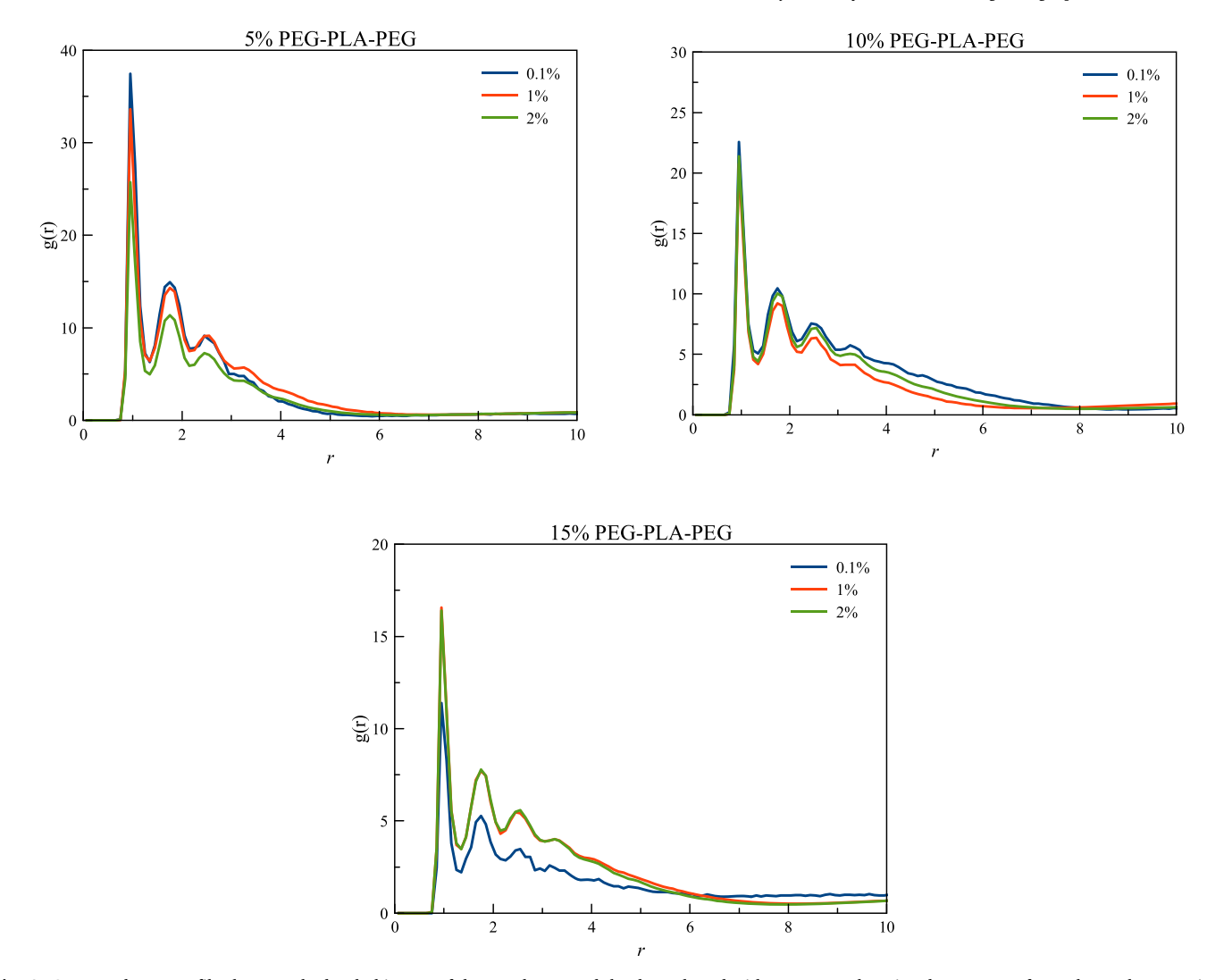


Fig. 4. Computed RDF profiles between hydrophobic part of the copolymer and the drug plotted with respect to changing drug content for each copolymer ratio in the system for drug encapsulation simulations. Distances are in DPD units $r_{\rm DPD}$.

between micelles is constant and the micelle properties does not change over time. Therefore, micelle properties are computed by considering only the final snapshot.

There is a consistent increase in the number of chains forming a particular micelle in each case of drug-free, drug encapsulation and drug release simulations as the copolymer content in the simulation box increases. It is also noted that the presence of drug in the system also increases the $N_{\rm agg}$ value if the drug-free and drug-laden systems are compared except for the 5% system in the encapsulation simulation. As expected, there is an inverse correlation between the $N_{\rm agg}$ and number of micelles in our findings. For the drug-laden simulations, the number of micelles is, in general, lower than the drug-free simulations at all cases except for the 5% system. This discrepancy might explain the inconsistency in the decreasing $N_{\rm agg}$ value as the system is loaded with drug molecules at 5% copolymer content. Moreover, it is noted that even a portion of the drug has left the micelles (i.e., release simulations), the

 N_{agg} and N_{m} for the 10% and 15% systems remain similar to the encapsulation simulations.

Another property of micelles, is the average micelle volume associated with all of the systems. The micelle volumes are computed by considering the hydrophobic beads forming the core part. Hydrophilic tails (namely, corona section) of the micelles are somewhat scattered irregularly and less dense, which might lead to incorrect estimation of the correct volume. In Table 2, we report the average values of the micelle volumes for the micelles that are considered irrespective of their $N_{\rm agg}$ value since not all systems exhibit similar $N_{\rm agg}$ distribution.

As for the drug-free system, the increasing copolymer concentration led to enlarged volumes of micelles as clearly noted in Table 2. The same trend can be found in the 0.1% drug content of the drug encapsulation and 0.1% and 1% drug content of the release simulations. For the rest of the systems, there is some discrepancy in the micelle volumes since the average micelle volumes correspond to a wide range of mean

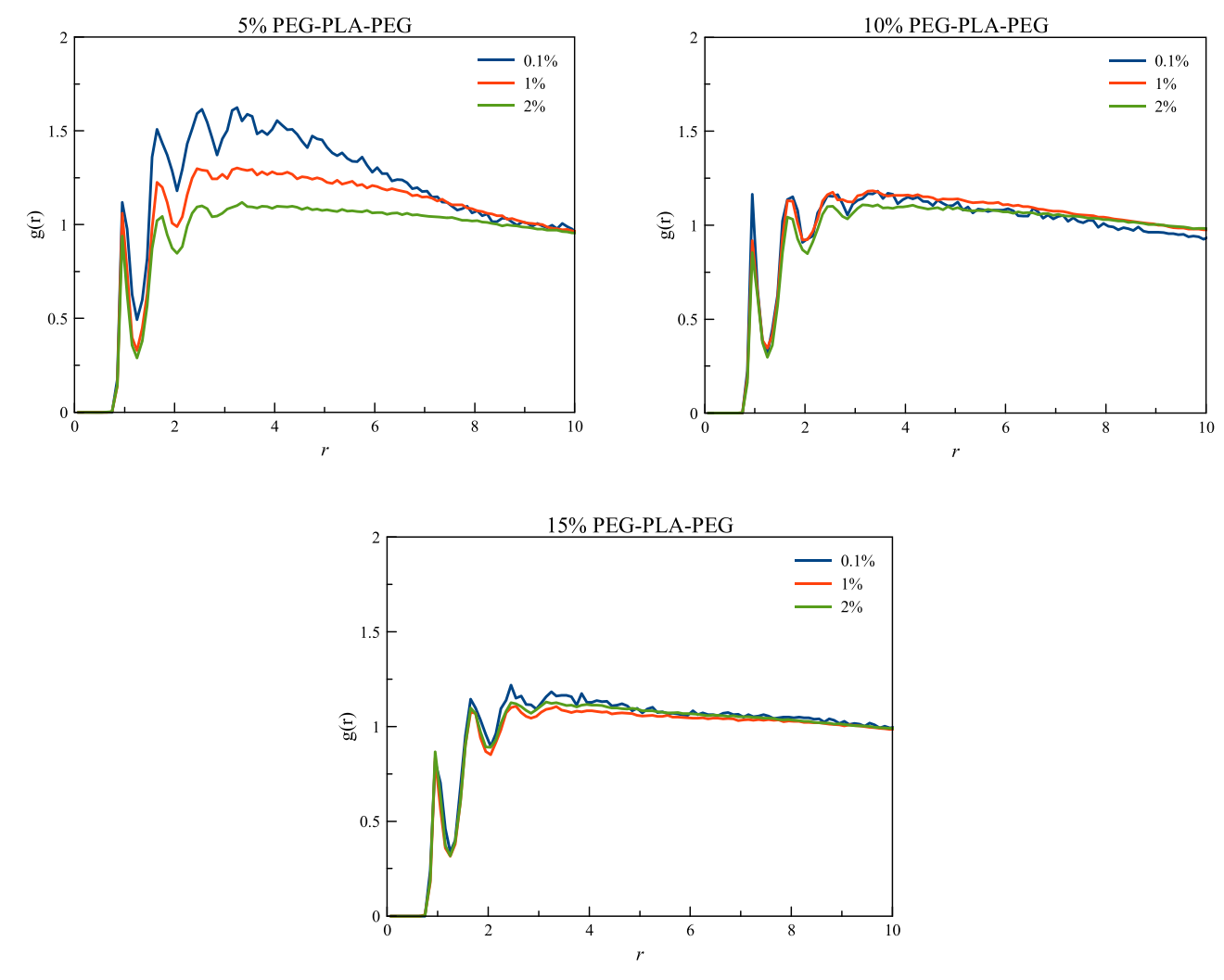


Fig. 5. Computed RDF profiles between hydrophilic part of the copolymer and the drug plotted with respect to changing drug content for each copolymer ratio in the system computed for drug release simulations. Distances are in DPD units $r_{\rm DPD}$.

aggregation number distribution. Moreover, the drug encapsulation leads to enlarging micelle volumes for the systems in general.

Finally, we calculate the relative shape anisotropy κ^2 as computed from the gyration tensor *S via* [71].

The relative shape anisotropy value converges to zero if the points are spherically symmetric and converges to one if all points lie on a line. Our computed κ^2 values in Table 3 shows us that the obtained micelles are very close to a spherical geometry. The values between different

$$S = \frac{1}{N} \begin{bmatrix} \sum_{i} (x_{i} - x_{cm})^{2} & \sum_{i} (x_{i} - x_{cm})(y_{i} - y_{cm}) & \sum_{i} (x_{i} - x_{cm})(z_{i} - z_{cm}) \\ \sum_{i} (x_{i} - x_{cm})(y_{i} - y_{cm}) & \sum_{i} (y_{i} - y_{cm})^{2} & \sum_{i} (y_{i} - y_{cm})(z_{i} - z_{cm}) \\ \sum_{i} (x_{i} - x_{cm})(z_{i} - z_{cm}) & \sum_{i} (y_{i} - y_{cm})(z_{i} - z_{cm}) & \sum_{i} (z_{i} - z_{cm})^{2} \end{bmatrix}$$

$$(7)$$

where, $x_{\rm cm}$, $y_{\rm cm}$, and $z_{\rm cm}$ are the center-of-mass (CoM) coordinate of a particular micelle. The eigenvalues λ_1 , λ_2 , λ_3 of the symmetrical matrix yields radius-of-gyration R_g via $R_g^2 = \lambda_1 + \lambda_2 + \lambda_3$. Hence, the relative shape anisotropy is defined in Eq. (8) and the results are tabulated in Table 3. All micelles are taken into consideration in the computation.

$$\kappa^2 \equiv 1 - 3 \frac{\lambda_1 \lambda_2 + \lambda_2 \lambda_3 + \lambda_1 \lambda_3}{\left(\lambda_1 + \lambda_2 + \lambda_3\right)^2}.$$
 (8)

systems have minor difference. The least and the most spherical micelles are obtained for 5% copolymer and 2% drug system at the encapsulation simulation, and release simulation for the same system, respectively. Overall, the presence of the hydrophobic drug leads to an increasing sphericity of the micelles. Even though some portion of the drug is released, the micelles still sustain their spherical morphology.

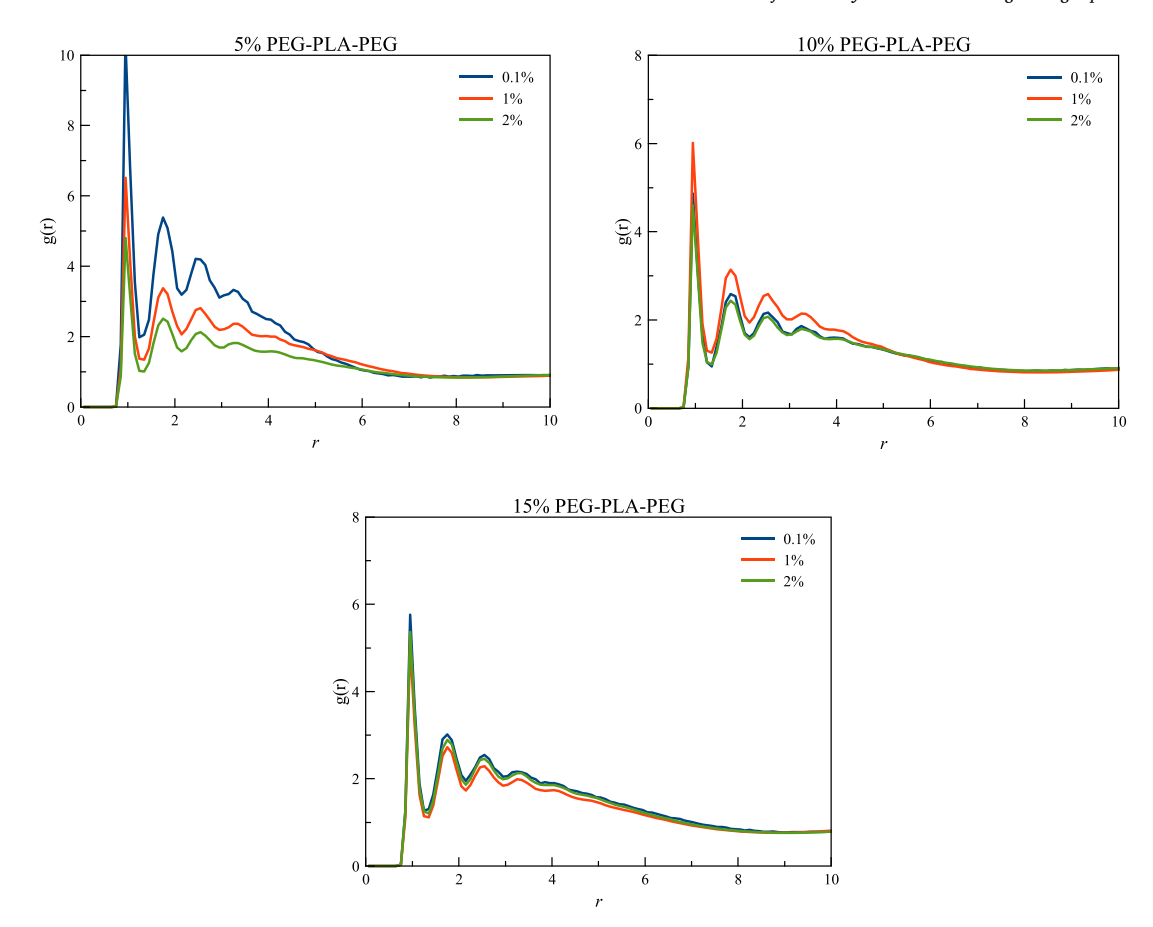


Fig. 6. Computed RDF profiles between hydrophobic part of the copolymer and the drug plotted with respect to changing drug content for each copolymer ratio in the system computed for drug release simulations. Distances are in DPD units r_{DPD} .

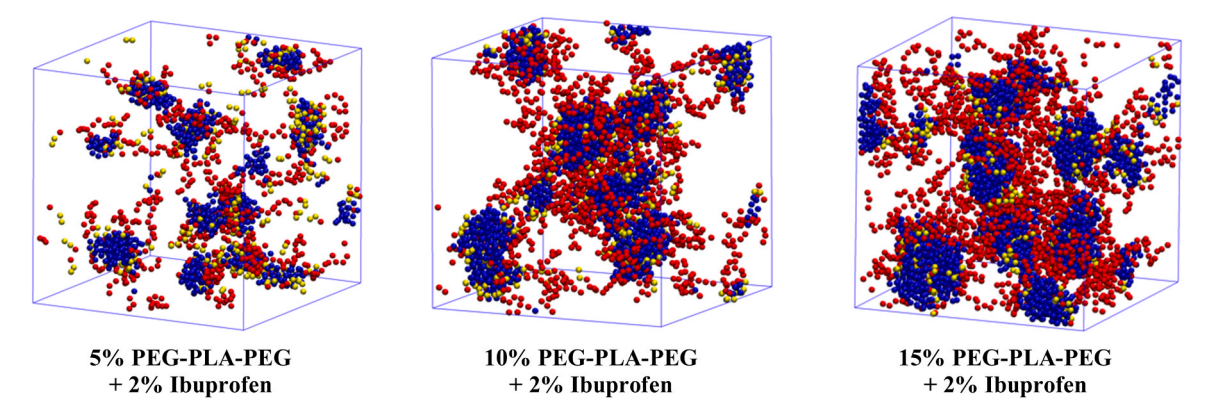
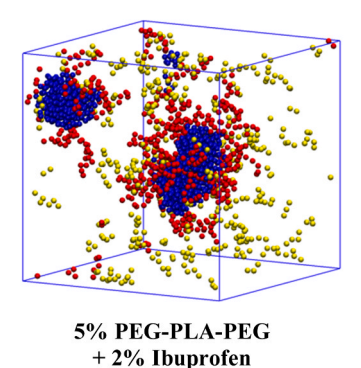


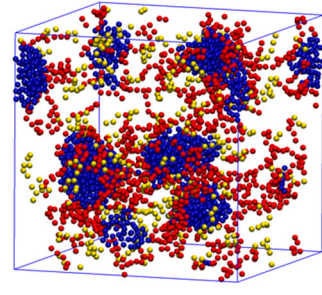
Fig. 7. Simulation snapshots of the micelles of 5%, 10% and 15% copolymer systems at 2% drug loading upon encapsulation of ibuprofen. For a better visualization, water molecules are not shown. Red and blue colors show hydrophilic and hydrophobic parts of the copolymer, respectively. Yellow color shows ibuprofen beads in this case. (For interpretation of the references to color in this figure legend, the reader is referred to the web version of this article.)

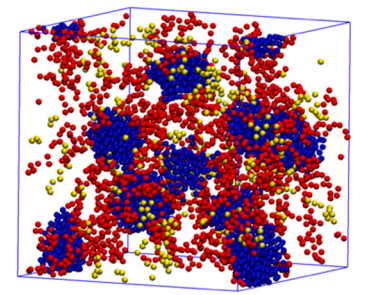
3.4. Quantifying drug encapsulation efficiencies as influenced by drug encapsulation and release

In this section, we compute the DEE values of the micelles as influenced by the drug encapsulation and release processes. The encapsulation efficiency values increase systematically as the copolymer concentration in the system is increased as shown in Fig. S4 of the Supplementary Material. In this figure, the DEE values of all systems fluctuate significantly around the mean value for low ibuprofen weight percent values (i.e., 0.1% drug loading) due to the poor statistics associated with the limited number of ibuprofen molecules in the mixtures.

The highest DEE values are obtained for the 15% copolymer system for all ibuprofen concentrations, which are almost independent of the loaded drug in the system. In contrast, the 0.1% ibuprofen loaded systems for the 5% and 10% copolymer systems are significantly lower compared to the 1% and 2% drug loading values. This result can be attributed to the decrease of the interactions between the hydrophobic and drug beads. In other words, as there is a lesser number of drug beads in the system, the chance that the hydrophobic and drug beads find each other is significantly low due to the short-range nature of DPD interactions. This is not the case for the 15% copolymer system since the copolymer beads occupy larger volumes in the simulation box, which







10% PEG-PLA-PEG + 2% Ibuprofen

15% PEG-PLA-PEG + 2% Ibuprofen

Fig. 8. Simulation snapshots of the micelles of 5%, 10% and 15% copolymer systems at 2% drug loading after the drug release process takes place. For a better visualization, water molecules are not shown. Red and blue colors show hydrophilic and hydrophobic parts of the copolymer, respectively. Yellow color shows ibuprofen beads. (For interpretation of the references to color in this figure legend, the reader is referred to the web version of this article.)

Table 2 Average micelle volume $V_{\rm m}$ computed for every simulated system. Only final snapshot is considered. The errors are the standard error of the mean.

	No drug	Encapsulation	Encapsulation			Release		
		0.1%	1%	2%	0.1%	1%	2%	
5%	171.2±26.5	134.6±19.7	423.2±50.7	223.5±49.7	282.8±43.4	357.2±13.3	406.5±54.9	
10%	237.7 ± 38.0	352.3 ± 34.3	363.2 ± 98.4	641.3 ± 99.9	$388.1 {\pm} 48.3$	$407.6 {\pm} 117.7$	516.8 ± 60.1	
15%	$302.8 {\pm} 58.2$	$383.1 {\pm} 71.0$	544.0 ± 69.6	558.1 ± 98.7	401.3 ± 63.7	500.3 ± 58.9	426.6 ± 59.2	

Table 3 The computed relative shape anisotropy κ^2 values. Only final snapshot is considered in the computation. The errors are the standard error of the mean.

	No drug	Encapsulation			Release		
		0.1%	1%	2%	0.1%	1%	2%
5%	0.095 ± 0.032	0.115 ± 0.033	$0.061{\pm}0.021$	0.119 ± 0.036	$0.022{\pm}0.006$	$0.021 {\pm} 0.011$	$0.007 {\pm} 0.002$
10%	$0.108 {\pm} 0.025$	$0.033{\pm}0.006$	$0.043{\pm}0.016$	$0.023{\pm}0.002$	$0.015{\pm}0.002$	$0.060 {\pm} 0.019$	$0.025 {\pm} 0.006$
15%	$0.062{\pm}0.017$	$0.051 {\pm} 0.013$	$0.028{\pm}0.006$	$0.015 {\pm} 0.003$	$0.032{\pm}0.011$	$0.018 {\pm} 0.003$	$0.017{\pm}0.004$

Table 4

The percentage release values of ibuprofen associated with each simulated system. The percentage change is computed by taking the ratio of the number of released drug molecules to the total number of initially encapsulated drug molecules.

System composition	Initial DEE value	DEE value after release	% release
5% polymer + 0.1% ibuprofen	37.5	15.5	58.6
5% polymer + 1% ibuprofen	53.2	14.7	72.4
5% polymer + 2% ibuprofen	51.6	11.7	77.3
10% polymer + 0.1% ibuprofen	62.5	26.8	57.1
10% polymer + 1% ibuprofen	76.6	28.1	63.3
10% polymer + 2% ibuprofen	77.4	23.5	69.6
15% polymer + 0.1% ibuprofen	87.5	42.8	51.1
15% polymer + 1% ibuprofen	88.3	35.6	59.7
15% polymer + 2% ibuprofen	86.4	39.6	54.2

increases the possibility of interaction between drug beads and the hydrophobic groups. It is also noticed that the amount of encapsulation leads to increase in the average micelle volume. In other words, the increase in the DEE values corresponding to a particular copolymer concentration in a system leads to an increase in the average micelle volumes as tabulated in Table 2. On the other hand, we observe no effect of the drug release on the micelle sizes as there is not a significant change of $V_{\rm m}$ in the drug release simulations as compared to the encapsulation simulations. The lesser amount of drug beads within the micelles still contributes to the enlarged micelles as compared to drug-free simulations. The maximum DEE value observed in the simulations is about 88.3% for the 15% copolymer and 1% drug, and the minimum value is about 37.5% for the system containing 5% copolymer and 0.1% ibuprofen.

To discuss better the system-specific trends of the DEE values, we plot the DEE values in Fig. S5 in the Supplementary Material for the systems that are equilibrated after the drug release takes place. In all, the overwhelming attraction of the FN bead to water as a result of the deprotonation lead to the migration of a huge portion of drug molecules to the solvent environment. In Fig. S5, we notice that in all combinations of the copolymer and the drug, there is a significant decrease in the total DEE values as compared to the initially encapsulated amount. Especially, for the 5% and 10% copolymer systems the final DEE values after

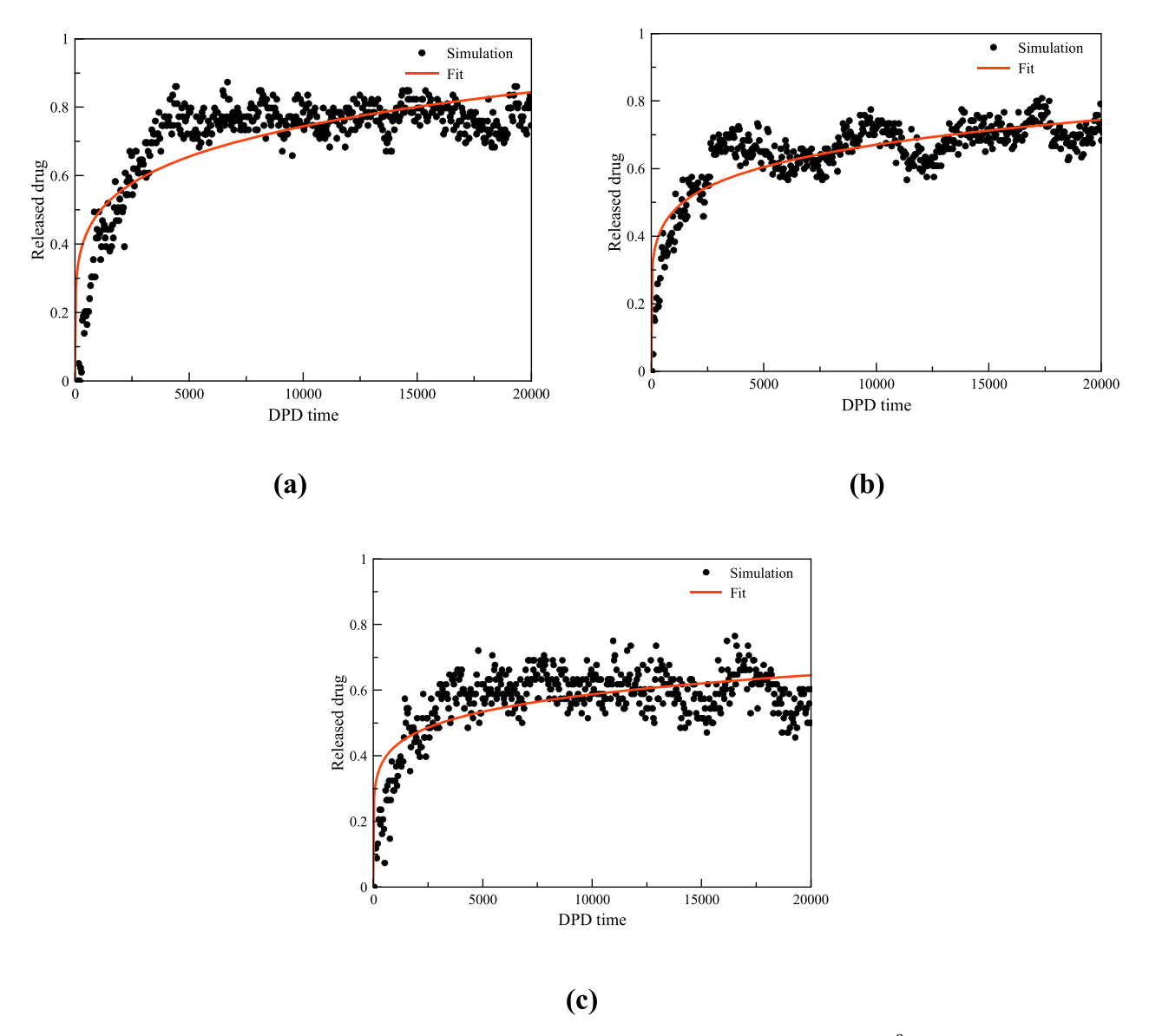


Fig. 9. The ibuprofen release profiles as a function of DPD time for (a) 5% copolymer + 2% drug (k = 0.1385, n = 0.1825, $R^2 = 0.6618$) (b) 10% copolymer + 2% drug (k = 0.1683, n = 0.1501, $R^2 = 0.6938$) and (b) 15% copolymer + 1% drug (k = 0.1670, n = 0.1365, $R^2 = 0.4885$) systems. The red line is the power-law fit to the simulation data representing Korsmeyer-Peppas release model [72,73].

the release process is obtained are almost independent of the drug loading in the system in contrast to their drug encapsulation simulations. There is a minor difference for the 15% copolymer system at the 1% drug loading, which is somewhat lower than the final DEE values of 0.1% and 2% systems. Nevertheless, the difference in the computed DEE values after the release can be considered as minor.

In Table 4, we quantify the percentage drug release of each system to comment on the different DEE behaviors of Fig. S4 and Fig. S5. It is observed that the difference between the drug release percentage values of the 5% and 10% systems at their 0.1% drug loadings are much lower compared to their 1% and 2% drug loading simulations. This might explain the change of the DEE profiles from encapsulation to release simulations, since more percentage release means a lower DEE value leading to a levelling off of their curves in Fig. S5. Overall, the system with the maximum release corresponds to 5% copolymer and 2% drug loaded system with a release amount of 77.3%. This means that 77.3% of the drug molecules that are initially encapsulated are released to the solvent environment. The drug release ratios for the rest of the systems can be found in Table 4.

3.5. Drug release kinetics

The time dependency of the drug release process is an important aspect of the drug release process. To characterize the ibuprofen release, we plot the fraction of the released drugs from the micelles as a function of the simulation time. To that purpose, we plot in Fig. 9, the systems with the highest DEE release ratio among a particular copolymer fraction, namely 5% copolymer $+\,2\%$ drug, 10% copolymer $+\,2\%$ drug and 15% copolymer $+\,1\%$ drug.

The drug release profiles in Fig. 9 are investigated by fitting a Korsmeyer-Peppas release model [72,73] to comment on the drug release behavior and compare the data with the existing release models. In the Korsmeyer-Peppas model, the fit is in the form of $C(t)/C_{\infty} = kt_{DPD}^n$, where $C(t)/C_{\infty}$ is the fraction of the drug release at a specific time, k is the rate constant and n is the release exponent. The fit parameters are obtained as indicated in the caption of Fig. 9.

As clearly noticed in Fig. 9, the drug release data is somewhat scattered due to the limited number of drug molecules in the simulation box. The scattered data means that the some of the ibuprofen beads move in

Table 5Computed diffusion constants *D* of ibuprofen beads for all simulated systems.

$D [r_{DPD}^2/t_{DPD}]$	Encapsulation		Release			
	0.1%	1%	2%	0.1%	1%	2%
5%	0.413	0.557	0.145	0.263	0.425	0.454
10%	0.265	0.245	0.241	0.233	0.361	0.373
15%	0.173	0.208	0.147	0.497	0.567	0.291

and out of the micelles during the simulations. The cyclic profile observed especially in Fig. 9(b) indicates that there is a competition for some drug molecules to be present inside the micelles or in the solvent environment. Nevertheless, once drugs are released, most of the drug molecules stays inside the solvent at all times during the simulation. The simulation times are much lower compared to the real experimental time-scales. Therefore, we evaluate our simulation data by assuming that the system is in quasi-equilibrium.

The exponent values n obtained for all of the cases in Fig. 9 are below the threshold value for Korsmeyer-Peppas model for Fickian diffusion (n = 0.5) [73]. Therefore, we can comment that the drug release behavior dictates an initial burst release followed by a diffusion indicating that the drug release is mainly governed by a pseudo-Fickian diffusion model [74]. As noted previously, the drug release takes place as a result of the increase in the relative affinity of carboxylate groups to water compared to the carboxyl group of the ibuprofen molecule. During the drug release, the micelles are observed to remain intact at all times and as discussed previously, the extent of the drug release is heavily influenced by crowding of the simulation box. Our systems are composed of multiple micelles and the simulation box dimensions are limited, which eventually slows down the drug diffusion to the water medium. In the case of a single micelle, the extent of drug release could go up to 100% as noted in literature [75,76]. Moreover, the rupture of the micelles that are observed during in vivo drug delivery as a result of the external mechanical forces that act on the copolymeric micelles is another effect, which might enhance the released drug amount.

The diffusion of drug molecules in the simulation box gives us an estimate of the average mobility and the diffusion rate of these beads. The mean squared displacement (MSD) $\langle \Delta r^2(t) \rangle$ is computed as $\langle \Delta r^2(t) \rangle = \langle |r_i(t) - r_i(0)|^2 \rangle$, where $r_i(t)$ is the position of a particle at time t, and $\langle \bullet \bullet \bullet \rangle$ represents the particle average. The slope of the MSD is proportional to the diffusion constant D via $D = \lim_{t \to \infty} \frac{1}{6t} \langle \Delta r^2(t) \rangle$. In our work, we compute the diffusion constants of ibuprofen beads for every system as shown in Table 5 from the computed MSD profiles.

The *D* values in Table 5 yields in general an increasing diffusion of drug beads in the release simulations as compared to the encapsulation simulations. Higher mobility values in the release simulations are expected due to the relocation of ibuprofen beads from the micelles to the aqueous environment. Nevertheless, a significant slowing down in the mobility of the released drug beads is observed in the 5% copolymer content at 0.1% and 1% drug loadings, being the former has the highest rate of decrease. The former system is noted in Table 5 as the system with an increasing number of micelles in the encapsulation simulations as compared to drug-free and drug release simulations. The increase in the number of micelles might lead to a slowing down of ibuprofen diffusion due to an increasing probability of interaction of a particular ibuprofen bead with copolymer micelles.

4. Conclusions

In this work, we employ coarse-grained DPD simulations with an alternative parameterization that incorporates the bead-size differences and hydrogen bond attraction to study the morphologies, drug encapsulation and drug release properties of PEG-PLA-PEG copolymer systems. Moreover, the micellar structures are characterized by means of

the mean aggregation number, average micelle volume and the relative shape anisotropy values. As a result of our simulations, the micelles are found to have high sphericity and observed to agree well with the experimental results of the same system [29]. Moreover, the encapsulation of the drug is noted to increase the micelle sizes and mean aggregation number. By changing the copolymer and drug concentration, we observe difference in the drug encapsulation efficiency values. The release process of ibuprofen from the micelles is modeled by mimicking the realistic experimental conditions, where carboxyl group of ibuprofen is deprotonated upon existence in the physiological conditions. As a consequence, the water affinity of ibuprofen is increased by assigning a significantly higher value of hydrogen bond strength to the corresponding carboxylate bead. By this procedure, we study the effect of the drug release on the structure and the copolymer and drug interactions. Hence, we find that the local interactions and structure of the copolymer and the drug is correlated with the extent of the drug release, where their interactions decrease as higher amount of drug beads are released from the micelles. We also conclude that the extent of the drug release is influenced by the crowding of the simulation box by the copolymer chains. Finally, the ibuprofen release dynamics are studied and observed that the release can be represented by a pseudo-Fickian diffusion model as revealed by a fitting of the drug release rate to the Korsmeyer-Peppas release model. Moreover, an increase in the diffusion rate of drug beads is noted in the drug release simulations as compared to the drug encapsulation simulations. In all, our work stands out as a realistic computational procedure to study the copolymer concentration dependent morphologies, drug encapsulation and drug release from a particular self-assembled copolymer micelle system, while bringing new insights on its molecular and micelle structure and their dependence on the drug encapsulation and release properties. Moreover, the computational procedure presented in this paper can be considered as a tool to direct the design of prospective drug delivery micelles with the aim to increase in vivo circulation of the hydrophobic drugs.

CRediT authorship contribution statement

MMK: Conceptualization, data curation, formal analysis, investigation, software, visualization, writing – original draft. EAD: Conceptualization, data curation, formal analysis, investigation, methodology, resources, validation. GK: Conceptualization, data curation, formal analysis, funding acquisition, project administration, supervision, writing – original draft, writing – review & editing.

Declaration of Competing Interest

There are no conflicts of interest to declare.

Acknowledgments

The simulations reported in this work were partially performed at TUBITAK ULAKBIM, High Performance and Grid Computing Center (TRUBA resources). GK would like to thank for the financial support from Trakya University Research Fund (no. 2020/108).

Appendix A. Supporting information

Supplementary data associated with this article can be found in the online version at doi:10.1016/j.colsurfa.2021.127445.

References

- V.P. Torchilin, Micellar nanocarriers: pharmaceutical perspectives, Pharm. Res. 24 (2007) 1–16.
- [2] J.K. Patra, G. Das, L.F. Fraceto, E.V.R. Campos, M.D.P. Rodriguez-Torres, L. S. Acosta-Torres, L.A. Diaz-Torres, R. Grillo, M.K. Swamy, S. Sharma, S. Habtemariam, H.S. Shin, Nano based drug delivery systems: recent developments and future prospects, J. Nanobiotechnol. 16 (2018) 71.

- [3] M. Estanqueiro, M.H. Amaral, J. Conceicao, J.M.S. Lobo, Nanotechnological carriers for cancer chemotherapy: the state of the art, Colloid Surf. B 126 (2015) 631–648
- [4] R. Langer, Drug delivery and targeting, Nature 392 (1998) 5-10.
- [5] D. Peer, J.M. Karp, S. Hong, O.C. FaroKHzad, R. Margalit, R. Langer, Nanocarriers as an emerging platform for cancer therapy, Nat. Nanotechnol. 2 (2007) 751–760.
- [6] T.M. Allen, P.R. Cullis, Liposomal drug delivery systems: from concept to clinical applications, Adv. Drug Deliv. Rev. 65 (2013) 36–48.
- [7] N.A. Peppas, J.Z. Hilt, A. Khademhosseini, R. Langer, Hydrogels in biology and medicine: from molecular principles to bionanotechnology, Adv. Mater. 18 (2006) 1345–1360.
- [8] D. Xiao, H.Z. Jia, J. Zhang, C.W. Liu, R.X. Zhuo, X.Z. Zhang, A dual-responsive mesoporous silica nanoparticle for tumor-triggered targeting drug delivery, Small 10 (2014) 591–598.
- [9] S. Sharma, A. Verma, B.V. Teja, G. Pandey, N. Mittapelly, R. Trivedi, P.R. Mishra, An insight into functionalized calcium based inorganic nanomaterials in biomedicine: trends and transitions, Colloid Surf. B 133 (2015) 120–139.
- [10] R. Duncan, The dawning era of polymer therapeutics, Nat. Rev. Drug Discov. 2 (2003) 347–360.
- [11] V.P. Torchilin, Structure and design of polymeric surfactant-based drug delivery systems, J. Control Release 73 (2001) 137–172.
- [12] E.S. Lee, Y.T. Oh, Y.S. Youn, M. Nam, B. Park, J. Yun, J.H. Kim, H.T. Song, K.T. Oh, Binary mixing of micelles using Pluronics for a nano-sized drug delivery system, Colloid Surf. B 82 (2011) 190–195.
- [13] D.J. Bharali, S.K. Sahoo, S. Mozumdar, A. Maitra, Cross-linked polyvinylpyrrolidone nanoparticles: a potential carrier for hydrophilic drugs, J. Colloid Interface Sci. 258 (2003) 415–423.
- [14] S. Mura, J. Nicolas, P. Couvreur, Stimuli-responsive nanocarriers for drug delivery, Nat. Mater. 12 (2013) 991–1003.
- [15] D.A. LaVan, T. McGuire, R. Langer, Small-scale systems for in vivo drug delivery, Nat. Biotechnol. 21 (2003) 1184–1191.
- [16] G. Kacar, Thermodynamic stability of ibuprofen loaded poloxamer micelles, Chem. Phys. 533 (2020), 110713.
- [17] S.C. Owen, D.P.Y. Chan, M.S. Shoichet, Polymeric micelle stability, Nano Today 7 (2012) 53–65.
- [18] M.A. Phillips, M.L. Gran, N.A. Peppas, Targeted nanodelivery of drugs and diagnostics, Nano Today 5 (2010) 143–159.
- [19] S. Biswas, P. Kumari, P.M. Lakhani, B. Ghosh, Recent advances in polymeric micelles for anti-cancer drug delivery, Eur. J. Pharm. Sci. 83 (2016) 184–202.
- [20] A. De Nicola, S. Hezaveh, Y. Zhao, T. Kawakatsu, D. Roccatano, G. Milano, Micellar drug nanocarriers and biomembranes: how do they interact? Phys. Chem. Chem. Phys. 16 (2014) 5093–5105.
- [21] Y. Wang, S. Tu, A.N. Pinchuk, M.P. Xiong, Active drug encapsulation and release kinetics from hydrogel-in-liposome nanoparticles, J. Colloid Interface Sci. 406 (2013) 247–255.
- [22] K. Yasugi, Y. Nagasaki, M. Kato, K. Kataoka, Preparation and characterization of polymer micelles from poly(ethylene glycol)-poly(D,L-lactide) block copolymers as potential drug carrier, J. Control Release 62 (1999) 89–100.
- [23] S.E.A. Gratton, P.A. Ropp, P.D. Pohlhaus, J.C. Luft, V.J. Madden, M.E. Napier, J. M. DeSimone, The effect of particle design on cellular internalization pathways, Proc. Natl. Acad. Sci. USA 105 (2008) 11613–11618.
- [24] S.R. Croy, G.S. Kwon, Polymeric micelles for drug delivery, Curr. Pharm. Des. 12 (2006) 4669–4684.
- [25] H. Maeda, Macromolecular therapeutics in cancer treatment: The EPR effect and beyond, J. Control Release 164 (2012) 138–144.
- [26] P. Grossen, D. Witzigmann, S. Sieber, J. Huwyler, PEG-PCL-based nanomedicines: a biodegradable drug delivery system and its application, J. Control Release 260 (2017) 46–60
- [27] A.M. Bodratti, P. Alexandridis, Formulation of poloxamers for drug delivery, J. Funct. Biomater. 9 (2018).
- [28] C.Z. Ding, Z.B. Li, A review of drug release mechanisms from nanocarrier systems, Mater. Sci. Eng. C-Mater. 76 (2017) 1440–1453.
- [29] X. Wu, S.M. Li, F. Coumes, V. Darcos, J.L.K. Him, P. Bron, Modeling and self-assembly behavior of PEG-PLA-PEG triblock copolymers in aqueous solution, Nanoscale 5 (2013) 9010–9017.
- [30] T. Yamaoka, Y. Tabata, Y. Ikada, Distribution and Tissue Uptake of Poly(Ethylene Glycol) with Different Molecular-Weights after Intravenous Administration to Mice, J. Pharm. Sci. 83 (1994) 601–606.
- [31] K.M. Nampoothiri, N.R. Nair, R.P. John, An overview of the recent developments in polylactide (PLA) research, Bioresour. Technol. 101 (2010) 8493–8501.
- [32] M. Chansuna, N. Pimpha, V. Vao-soongnern, Mesoscale simulation and experimental studies of self-assembly behavior of a PLA-PEG-PLA triblock copolymer micelle for sustained drug delivery, J. Polym. Res. 21 (2014) 452.
- [33] H. Danafar, K. Rostamizadeh, S. Davaran, M. Hamidi, Drug-conjugated PLA-PEG-PLA copolymers: a novel approach for controlled delivery of hydrophilic drugs by micelle formation, Pharm. Dev. Technol. 22 (2017) 947–957.
- [34] M.E. El-Naggar, F. Al-Joufi, M. Anwar, M.F. Attia, M.A. El-Bana, Curcumin-loaded PLA-PEG copolymer nanoparticles for treatment of liver inflammation in streptozotocin-induced diabetic rats, Colloid Surf. B 177 (2019) 389–398.
- [35] R. Gref, M. Luck, P. Quellec, M. Marchand, E. Dellacherie, S. Harnisch, T. Blunk, R. H. Muller, 'Stealth' corona-core nanoparticles surface modified by polyethylene glycol (PEG): influences of the corona (PEG chain length and surface density) and of the core composition on phagocytic uptake and plasma protein adsorption, Colloid Surf. B 18 (2000) 301–313.
- [36] P. Posocco, M. Fermeglia, S. Pricl, Morphology prediction of block copolymers for drug delivery by mesoscale simulations, J. Mater. Chem. 20 (2010) 7742–7753.

- [37] D.S. Dolgov, T.E. Grigor'ev, A.I. Kulebyakina, E.V. Razuvaeva, R.A. Gumerov, S. N. Chvalun, I.I. Potemkin, Aggregation in biocompatible linear block copolymers: computer simulation study, Polym. Sci. Ser. A 60 (2018) 902–910.
- [38] Y.H. Feng, X.P. Zhang, Z.Q. Zhao, X.D. Guo, Dissipative particle dynamics aided design of drug delivery systems: a review, Mol. Pharm. 17 (2020) 1778–1799.
- [39] M. Ramezani, J. Shamsara, Application of DPD in the design of polymeric nanomicelles as drug carriers, J. Mol. Graph Model. 66 (2016) 1–8.
- [40] S.J. Zeng, X.B. Quan, H.L. Zhu, D.L. Sun, Z.H. Miao, L.Z. Zhang, J. Zhou, Computer simulations on a pH-responsive anticancer drug delivery system using zwitteriongrafted polyamidoamine dendrimer unimolecular micelles, Langmuir 37 (2021) 1225–1234.
- [41] D. Xiong, X.F. Zhang, S.Y. Peng, H.W. Gu, L.J. Zhang, Smart pH-sensitive micelles based on redox degradable polymers as DOX/GNPs carriers for controlled drug release and CT imaging, Colloid Surf. B 163 (2018) 29–40.
- [42] W.F. Min, D.H. Zhao, X.B. Quan, D.L. Sun, L.B. Li, J. Zhou, Computer simulations on the pH-sensitive tri-block copolymer containing zwitterionic sulfobetaine as a novel anti-cancer drug carrier, Colloid Surf. B 152 (2017) 260–268.
- [43] C.F. Yang, Z.L. Xue, Y.L. Liu, J.Y. Xiao, J.R. Chen, L.J. Zhang, J.W. Guo, W.J. Lin, Delivery of anticancer drug using pH-sensitive micelles from triblock copolymer MPEG-b-PBAE-b-PLA, Mater. Sci. Eng. C-Mater. 84 (2018) 254–262.
- [44] G. Kacar, E.A.J.F. Peters, G. de With, Mesoscopic simulations for the molecular and network structure of a thermoset polymer, Soft Matter 9 (2013) 5785–5793.
- [45] G. Kacar, E.A.J.F. Peters, G. de With, A generalized method for parameterization of dissipative particle dynamics for variable bead volumes, EPL (Europhys. Lett.) 102 (2013) 40009.
- [46] G. Kacar, G. de With, Hydrogen bonding in DPD: application to low molecular weight alcohol-water mixtures, Phys. Chem. Chem. Phys. 18 (2016) 9554–9560.
- [47] P.J. Hoogerbrugge, J.M.V.A. Koelman, Simulating microscopic hydrodynamic phenomena with dissipative particle dynamics, Eur. Lett. 19 (1992) 155–160.
- [48] U. Frisch, B. Hasslacher, Y. Pomeau, Lattice-gas automata for the Navier-Stokes equation, Phys. Rev. Lett. 56 (1986) 1505–1508.
- [49] R.D. Groot, P.B. Warren, Dissipative particle dynamics: bridging the gap between atomistic and mesoscopic simulation, J. Chem. Phys. 107 (1997) 4423–4435.
- [50] P.J. Flory, Principles of Polymer Chemistry, Cornell University Press, Ithaca, New York, 1953.
- [51] M.B. Liu, G.R. Liu, L.W. Zhou, J.Z. Chang, Dissipative Particle Dynamics (DPD): an overview and recent developments, Arch. Comput. Method E 22 (2015) 529–556.
- [52] G. Kacar, G. de With, Parametrizing hydrogen bond interactions in dissipative particle dynamics simulations: the case of water, methanol and their binary mixtures, J. Mol. Liq. 302 (2020), 112581.
- [53] K. Marushkevich, L. Khriachtchev, M. Rasanen, Hydrogen bonding between formic acid and water: Complete stabilization of the intrinsically unstable conformer, J. Phys. Chem. A 111 (2007) 2040–2042.
- [54] G. Kacar, Molecular understanding of interactions, structure, and drug encapsulation efficiency of Pluronic micelles from dissipative particle dynamics simulations, Colloid Polym. Sci. 297 (2019) 1037–1051.
- [55] S. Evoli, D.L. Mobley, R. Guzzi, B. Rizzuti, Multiple binding modes of ibuprofen in human serum albumin identified by absolute binding free energy calculations, Phys. Chem. Chem. Phys. 18 (2016) 32358–32368.
- [56] P.A. Sigala, E.A. Ruben, C.W. Liu, P.M.B. Piccoli, E.G. Hohenstein, T.J. Martinez, A. J. Schultz, D. Herschlag, Determination of hydrogen bond structure in water versus aprotic environments to test the relationship between length and stability, J. Am. Chem. Soc. 137 (2015) 5730–5740.
- [57] O. Markovitch, N. Agmon, Structure and energetics of the hydronium hydration shells, J. Phys. Chem. A 111 (2007) 2253–2256.
- [58] T. Urbic, Ions increase strength of hydrogen bond in water, Chem. Phys. Lett. 610 (2014) 159–162.
- [59] X.Q. Sun, S. Yoo, S.S. Xantheas, L.X. Dang, The reorientation mechanism of hydroxide ions in water: a molecular dynamics study, Chem. Phys. Lett. 481 (2009) 0.16
- [60] K. Stoyanova, Z. Vinarov, S. Tcholakova, Improving Ibuprofen solubility by surfactant-facilitated self-assembly into mixed micelles, J. Drug Deliv. Sci. Technol. 36 (2016) 208–215.
- [61] LAMMPS Simulator, $\langle http://lammps.sandia.gov \rangle$, 2020.
- [62] S. Plimpton, Fast parallel algorithms for short-range molecular-dynamics, J. Comput. Phys. 117 (1995) 1–19.
- [63] Scienomics MAPS v4.4, (http://www.scienomics.com), 2018.
- [64] H. Droghetti, I. Pagonabarraga, P. Carbone, P. Asinari, D. Marchisio, Dissipative particle dynamics simulations of tri-block co-polymer and water: phase diagram validation and microstructure identification, J. Chem. Phys. 149 (2018), 184903.
- [65] R.D. Groot, K.L. Rabone, Mesoscopic simulation of cell membrane damage, morphology change and rupture by nonionic surfactants, Biophys. J. 81 (2001) 725–736.
- [66] X.H. Wu, A. El Ghzaoui, S.M. Li, Anisotropic self-assembling micelles prepared by the direct dissolution of PLA/PEG block copolymers with a high PEG fraction, Langmuir 27 (2011) 8000–8008.
- [67] A. Vishnyakov, M.T. Lee, A.V. Neimark, Prediction of the critical micelle concentration of nonionic surfactants by dissipative particle dynamics simulations, J. Phys. Chem. Lett. 4 (2013) 797–802.
- [68] R.L. Anderson, D.J. Bray, A. Del Regno, M.A. Seaton, A.S. Ferrante, P.B. Warren, Micelle formation in alkyl sulfate surfactants using dissipative particle dynamics, J. Chem. Theory Comput. 14 (2018) 2633–2643.
- [69] R. Basak, R. Bandyopadhyay, Encapsulation of hydrophobic drugs in pluronic F127 micelles: effects of drug hydrophobicity, solution temperature, and pH, Langmuir 29 (2013) 4350–4356.

- [70] H. Almeida, P. Lobao, C. Frigerio, J. Fonseca, R. Silva, J.M.S. Lobo, M.H. Amaral, Preparation, characterization and biocompatibility studies of thermoresponsive eyedrops based on the combination of nanostructured lipid carriers (NLC) and the polymer Pluronic F-127 for controlled delivery of ibuprofen, Pharm. Dev. Technol. 22 (2017) 336–349.
- [71] W.L. Mattice, U.W. Suter, Conformational Theory of Large Molecules: The Rotational Isomeric State Model in Macromolecular Systems, Wiley Interscience, New York, 1994.
- [72] P.L. Ritger, N.A. Peppas, A simple equation for description of solute release II. Fickian and anomalous release from swellable devices, J. Control Release 5 (1987) 37-42
- [73] R.W. Korsmeyer, R. Gurny, E. Doelker, P. Buri, N.A. Peppas, Mechanisms of solute release from porous hydrophilic polymers, Int J. Pharm. 15 (1983) 25–35.
- [74] M. Srivastava, K. Kohli, M. Ali, Formulation development of novel in situ nanoemulgel (NEG) of ketoprofen for the treatment of periodontitis, Drug Deliv. 23 (2016) 154–166.
- [75] L. Jia, R. Wang, Y.N. Fan, Encapsulation and release of drug nanoparticles in functional polymeric vesicles, Soft Matter 16 (2020) 3088–3095.
- [76] W.J. Lin, Z.L. Xue, L.Y. Wen, Y.Z. Li, Z.P. Liang, J.C. Xu, C.F. Yang, Y.X. Gu, J. Zhang, X.H. Zu, H.S. Luo, G.B. Yi, L.J. Zhang, Mesoscopic simulations of drugloaded diselenide crosslinked micelles: stability, drug loading and release properties, Colloids Surf. B Biointerfaces 182 (2019), 110313.